

SEARCHING FOR LUNAR TIDAL DEFORMATIONS WITH LOLA. M. K. Barker¹, E. Mazarico², G. A. Neumann³, D. E. Smith^{2,3}, M. T. Zuber² and the LOLA Science Team, ¹Sigma Space Corp., 4600 Forbes Blvd. Lanham, MD 20706 michael.barker@sigmaspace.com, ²Dept. of Earth, Atmospheric and Planetary Sciences, MIT, 77 Massachusetts Ave. Cambridge, MA 02139, ³Solar System Exploration Division, NASA Goddard Space Flight Center 8800 Greenbelt Rd. Greenbelt, MD 20771.

Introduction: The Moon exhibits a tidal gravity field due to the difference in the gravitational force of the Earth (and to a lesser extent, the Sun) at the Moon's surface and its center of mass. This field causes elastic changes to the solid body of the Moon. For example, the Moon is slightly squashed along the limb and bulged on the near and far sides with a maximum radial displacement of ~ 50 cm (with respect to a perfect sphere) near the sub-Earth point and its antipode. The detailed behavior of these deformations depends on the Moon's physical properties, such as the density distribution and bulk elastic properties, which are often parameterized in terms of the Love numbers. Therefore, the Moon's tidal gravity field has important consequences for areas of active research, like lunar geodesy, the interior structure of the Moon, and the long-term evolution of the Earth-Moon system [1].

The lunar tidal gravity field not only varies with position, but with time, as well. As the Moon revolves around the Earth it experiences changes in the gravitational force due to the orbital eccentricity and obliquity. These changes lead to radial variations about the mean tidal bulge shape with a dominant period of ~ 27.5 days and a peak-to-peak amplitude as large as ~ 20 cm at some surface locations (Figure 1). Thus, it should be possible to detect the signature of lunar tides

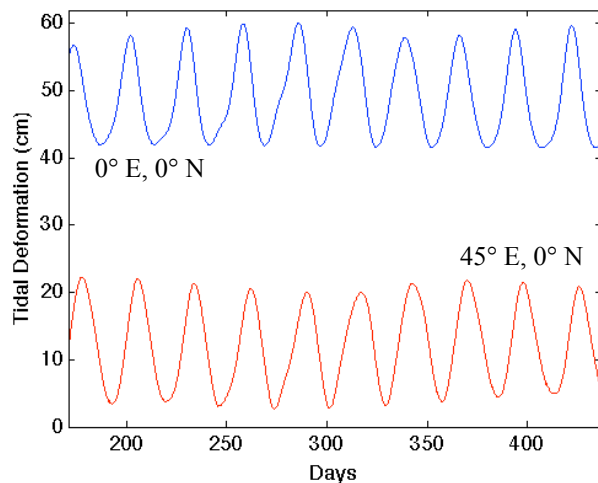


Figure 1 - Radial tidal deformation as a function of time for two points on the Moon's surface using the analytic formulae given by [2].

with repeated accurate measurements of the surface height at many different locations.

After ~ 3.5 years of operation, the Lunar Orbiter Laser Altimeter (LOLA) aboard the Lunar Reconnaissance Orbiter (LRO) has collected over 5.6 billion measurements of surface height with a vertical precision of ~ 10 cm and an accuracy of ~ 1 m. The LOLA dataset contains ~ 10 million crossovers, instances when two ground-tracks intersect. Previous work has demonstrated the utility of altimetric crossovers in improving reconstructed spacecraft orbits [3]. In the case of LOLA, these crossovers are especially useful because the 5-spot, 50-m wide footprint provides extra information in the cross-track direction [4]. This allows each track to form a 2-dimensional surface onto which the other track's footprints can be interpolated for comparison. Although the combined precision and accuracy of any single LOLA height measurement is larger than the expected tidal signal, with sufficiently large samples it may be possible to detect such a signal. In this contribution, we present preliminary results of efforts to use LOLA crossovers to detect the signature of tidal deformations.

Crossover Analysis: Each crossover is the intersection of two separate ground-tracks and, thus, represents two distinct measurements of the same surface location at two different times. Ideally, for a static surface and with no measurement errors, these measurements would yield the same height, but in reality the lunar surface is not completely static and the measurements are not completely error-free. As stated above, the Moon experiences changes in its tidal deformations as it revolves around the Earth. Errors in the LOLA altimetry arise primarily from our imperfect knowledge of the LRO orbit and LOLA orientation. Any difference in the height measurements at the intersection of a crossover are due largely to these effects.

The method for processing each LOLA crossover is similar to that in the work of [4], to which we refer the reader for a detailed explanation. Here we provide a brief overview. We restrict the analysis to those crossovers where both tracks have valid returns from all 5 spots. This reduces the number of usable crossovers to $\sim 600,000$ (Figure 2).

For each crossover, we solve for the best-fit offsets in the X, Y, and Z directions in a local stereographic

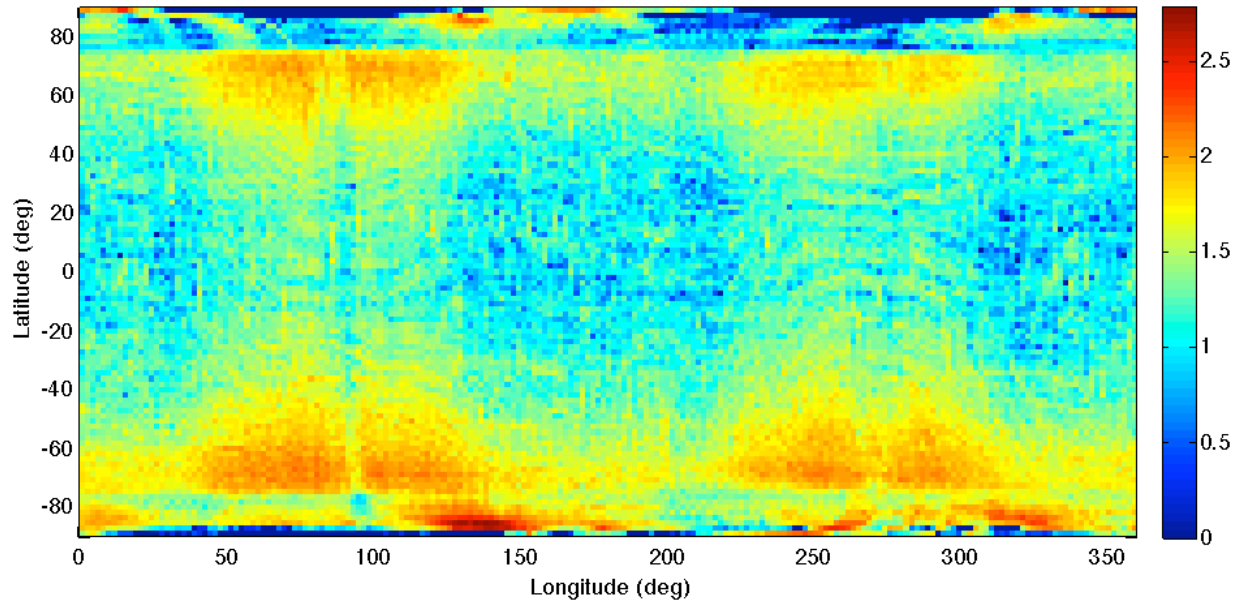


Figure 2 - Spatial density of crossovers on a logarithmic color scale and cylindrical projection.

frame centered on the intersection region. We also estimate the errors of the XYZ offsets by iteratively stepping away from the best-fit and recording where the reduced χ^2 changes by one. This allows us to identify and exclude potentially weak crossovers that have large errors. Figure 3 shows a typical crossover with a shallow intersection angle in stereographic projection. The vertical profiles of the same crossover are shown in Figure 4 after applying the best-fit offsets. The final RMS residual is 53 cm.

Future work will involve processing all crossovers in a similar manner and comparing the derived offsets

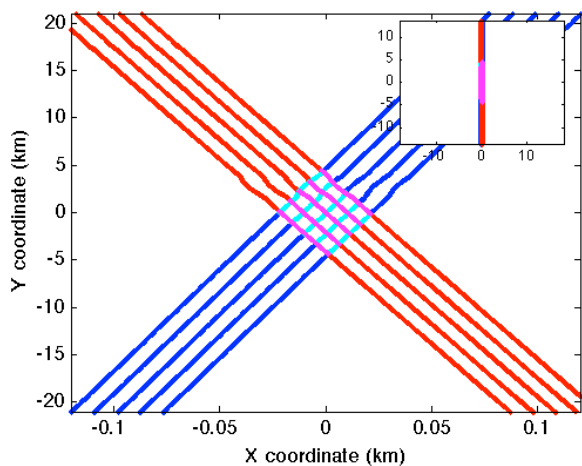


Figure 3 - A typical crossover with a shallow intersection angle in stereographic projection. Note the different scales of the x and y axes. For comparison, the inset has equal scaling of the axes. Points used in the fit evaluation are colored cyan and magenta.

to predictions for tidal deformations based on theoretical models of the lunar interior. We will also investigate solving directly for the best-fit Love numbers in a least-squares sense using the differences between the predicted and observed offsets. Finally, we expect the determination of the LRO orbit to continuously improve with updated GRAIL gravity models [5]. These improvements will be incorporated into the analysis.

References: [1] *Lunar Gravimetry*, ed. Sagitov, M. U. et al. London: Academic Pr., 1986. [2] Ooe, H. and Hanada, H. (1992) *JPE*, 40, 525-534. [3] Neumann, G. A. et al. (2001) *JGR*, 106, 23753-23768. [4] Mazarico, E. et al. (2010) *Jour. of Geod.*, 84, 343-354. [5] Zuber, M. T. et al. (2013) *Sci.* DOI: 10.1126/science.1231507.

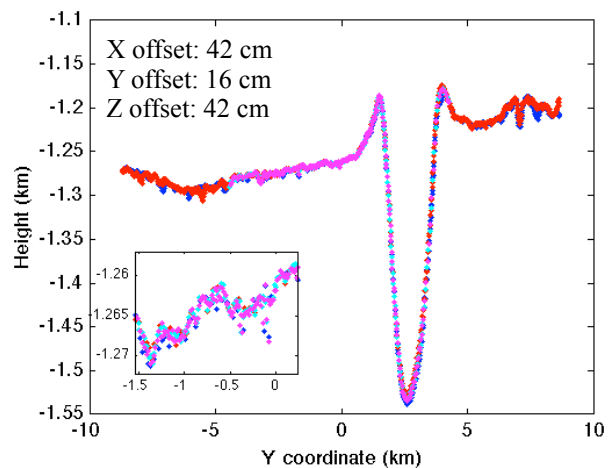


Figure 4 - Vertical profiles of crossover shown in Fig. 3 after applying best-fit offsets. Color coding of points is the same as in Fig. 3. Inset shows a close-up of one particular region.